Effect of Wigner rotation on estimating the unitary-shift parameter of a relativistic spin-1/2 particle

Shin Funada and Jun Suzuki

Graduate School of Informatics and Engineering, The University of Electro-Communication, 1-5-1 Chofugaoka, Chofu-shi, Tokyo 182-8585, Japan

(Received 12 May 2022; revised 30 September 2022; accepted 26 October 2022; published 5 December 2022)

We obtain the accuracy limit for estimating the expectation value of the position of a relativistic particle for an observer moving in one direction at a constant velocity. We use a specific model of a relativistic spin-1/2 particle described by a Gaussian wave function with a spin down in the rest frame. To derive the state vector of the particle for the moving observer, we use the Wigner rotation that entangles the spin and the momentum of the particle. Based on this wave function for the moving frame, we obtain the symmetric logarithmic derivative (SLD) Cramér-Rao bound that sets the estimation accuracy limit for an arbitrary moving observer. It is shown that estimation accuracy decreases monotonically in the velocity of the observer when the moving observer does not measure the spin degree of freedom. This implies that the estimation accuracy limit worsens with the observer's increasing velocity, but it is finite even in the relativistic limit. We derive the amount of this information loss by the exact calculation of the SLD Fisher information matrix in an arbitrary moving frame.

DOI: 10.1103/PhysRevA.106.062404

I. INTRODUCTION

Relativistic quantum information theory introduces a new direction of research in physics. The significance of the effect of the relativity on the quantum state is that the state vector for a moving observer changes depending on the motion of the observer while the physical state in the rest frame remains the same. As a natural consequence, information that the moving observer obtains changes depending on the motion of the moving observer since the state vector changes. There are studies of quantum information theory with relativity being taken into account. The studies in the realm of relativistic quantum information have increased in number. Here we briefly list some of them. First, the information paradox about black holes is now formulated in the framework of information theory (see recent reviews in [1,2]). Second, quantum information in a noninertial frame was investigated [3–7]. Third, the effect of relativity on Bell's inequality was studied. The degree of the violation of Bell's inequality was investigated [8–13]. The entropy changes due to the relativistic effect [14] and their effect on Bell's inequality were also studied, initially in [15].

Among these early studies about relativity and quantum information, Refs. [8–10,16,17] introduced the use of the Wigner rotation [18,19] into the realm of quantum information. As another example, the Wigner rotation is used to discuss the limitation given by a quantum entropy in the relativity domain [14]. The entanglement [16,20–27] and Bell's inequality [8,10,28] have also been discussed by using the Wigner rotation. The essence of the Wigner rotation is that it "rotates" the spin of the relativistic particle by the angle, which is a function of the momentum of the particle. Thus, the spin and the momentum couple in a nontrivial way that the Wigner rotation gives.

Based on the previous investigations in relativistic quantum information theory, it is natural to pose the following question: What is the effect of the Wigner rotation on parameter estimation of quantum states? To phrase it differently, we ask how the estimation accuracy changes for a moving observer. However, studies of the change in estimation accuracy that a moving observer undergoes are lacking. We demonstrate how estimation accuracy changes for the moving observer in the framework of the quantum estimation theory [29,30]. To obtain the limit of estimation accuracy as a function of the moving observer's velocity, we utilize the quantum Fisher information matrix, which enables us to quantify the accuracy limit. Among those quantum Fisher information matrices, we consider the symmetric logarithmic derivative (SLD) Fisher information matrix as an indicator of estimation accuracy. As the main result, we obtain the analytical expression of the SLD Fisher information matrix for an arbitrary moving observer in an integral form (29). This then sets the estimation accuracy limits between the observers in the rest and moving frames. To illustrate our result, we plot the relativistic effect on estimation accuracy in Fig. 4. Estimation accuracy obtained by the SLD Fisher information matrix is finite even at the relativistic limit where the velocity V approaches the speed of light. This suggests that estimation accuracy remains finite at the relativistic limit.

As for the model, we set up a specific pure-state model that describes a single spin-1/2 particle. A parametric model is defined by a two-parameter unitary shift model. We next consider an observer moving at a constant velocity in one direction with respect to the rest frame. The moving observer then makes a measurement to estimate the parameters encoded in the state without accessing the spin degree of freedom. Thus, our parameter model in the moving frame is given by the Wigner rotation followed by the partial trace over the spin. We investigate how estimation accuracy for the moving observer changes as a function of the velocity. In our study, the parameters correspond to the expectation value for the position of the particle. We evaluate the limits for the mean square error upon estimating the expectation value of the position operator by the SLD Cramér-Rao (CR) bound. We obtain analytically how much the accuracy decreases as a function of the velocity of the moving observer.

Before closing the Introduction, let us briefly remark on the earlier works of estimation theory in the relativistic domain. A seminal paper [31] triggered the study of parameter estimation in the relativity domain. The result provided insight into the quantum estimation theory in the relativistic domain. In their work the authors derived an uncertainty relation based on the restriction provided by the Lorentz invariance. They did not consider the change in estimation accuracy or the uncertainty relation by the Lorentz transformation. The other instance of parameter estimation of a relativistic quantum state is known as relativistic quantum metrology [32–35]. However, these studies do not address the question proposed in this paper.

The outline of this paper is as follows. In Sec. II our model is explained. The state in the rest frame is given. The state in the moving frame is derived by applying the Wigner rotation to the state in the rest frame. In Sec. III we explain our parameter estimation, which is given by the wave function derived by the Wigner rotation. We first evaluate the SLD CR bound in such a case that the moving observer does not have information about the degree of freedom of the spin state. We also comment on the other two possible cases. The SLD CR bounds are investigated by multiparameter estimation and given in analytical forms. In Sec. IV we discuss how the Wigner rotation changes the wave function and gives rise to the loss of information. We also mention the possible experimental realization. Section V gives a brief summary. Appendix A summarizes well-known facts about the Wigner rotation for a massive spin-1/2 particle. Most of the technical calculations are presented in Appendixes B–F.

II. MODEL

We assume that an observer moves along the z axis with a constant velocity V. We choose the z direction as the moving direction because we expect that this direction gives the most significant change in the rotation of spin as a massive relativistic spin-1/2 particle on the x-y plane [10]. We use natural units, i.e., $\hbar = 1$ and $c = 1$, unless otherwise stated. The mass of the particle is m. As a metric tensor $g_{\mu\nu}$, we choose $g_{\mu\nu} = (+1, -1, -1, -1)$.

A. State in the rest frame

The wave function of the particle is set as a Gaussian function of x and y with a plane wave on the z coordinate. For simplicity, we set the wave number, or the momentum, in the z direction as zero. To apply the Wigner rotation as described in [18,19], we mainly use the momentum representation in the following discussion.

The state of the particle is in a known pure state called a reference state. The reference state ρ_0 in the rest frame is

$$\rho_0 = |\Psi_\downarrow\rangle\langle\Psi_\downarrow|,$$

$$|\Psi_\downarrow\rangle = \int d^3p\,\varphi_0(p^1)\varphi_0(p^2)\delta(p^3)\,|\vec{p},\downarrow\rangle, \tag{1}$$

where $\delta(p^3)$ denotes the Dirac delta function to represent the plane wave in the z direction. The momentum vector $\vec{p}$ is a spatial part of the four-momentum p^μ, i.e., $\vec{p} = (p^1, p^2, p^3)$. The state vectors $|\vec{p},\downarrow\rangle$ and $|\vec{p},\uparrow\rangle$ are the momentum eigenstates with down and up spins, respectively. The $\varphi_0(p)$ is defined by the Gaussian function as

$$\varphi_0(p) = \frac{\kappa^{1/2}}{\pi^{1/4}}e^{-\kappa^2p^2/2}. \tag{2}$$

The κ determines the spread of the wave function in the coordinate representation, i.e., the spread of the wave function in the coordinate representation becomes broader as κ increases. In this paper we assume that the spread κ can be tuned arbitrarily.

A quantum parametric model is defined by a two-parameter unitary model as

$$\mathcal{M}_{\text{rest}} = \{\rho_\theta \mid \theta = (\theta_1, \theta_2) \subset \mathbb{R}^2\}, \tag{3}$$

where ρ_θ is generated by the momentum operators in the x and y directions $\hat{p}^1$ and $\hat{p}^2$, respectively,

$$\rho_\theta = U(\theta)\rho_0U^\dagger(\theta) = U(\theta)|\Psi_\downarrow\rangle\langle\Psi_\downarrow|U^\dagger(\theta), \tag{4}$$

with

$$U(\theta) = e^{-i\hat{p}^1\theta_1 - i\hat{p}^2\theta_2}. \tag{5}$$

The operator $\hat{p}^i$ ($i = 1, 2$) is the momentum operator of the ith component, i.e., $\hat{p}^i|\vec{p},\sigma\rangle = p^i|\vec{p},\sigma\rangle$ ($\sigma = \downarrow, \uparrow$). Let us define a state vector $|\Psi_\downarrow(\theta)\rangle$ as

$$|\Psi_\downarrow(\theta)\rangle = U(\theta)|\Psi_\downarrow\rangle$$
$$= \int d^3p\,\varphi_0(p^1)\varphi_0(p^2)\delta(p^3)e^{-ip^1\theta_1 - ip^2\theta_2}\,|\vec{p},\downarrow\rangle. \tag{6}$$

Then Eq. (4) is expressed as

$$\rho_\theta = |\Psi_\downarrow(\theta)\rangle\langle\Psi_\downarrow(\theta)|. \tag{7}$$

The physical implication of the parameter θ is that it is the peak position of the wave function in the coordinate representation. Alternatively, we consider position operators $\hat{x}^j$, which are canonical conjugates of the momentum operators $\hat{p}^j$ ($j = 1, 2$).[1] From Eq. (5) we have

$$U^\dagger(\theta)\hat{x}^jU(\theta) = \hat{x}^j + \theta_j \quad (j = 1, 2). \tag{8}$$

The unitary transformation $U(\theta)$ gives a shift by θ_j to a position operator $\hat{x}^j$. By assumption, we know the reference state ρ_0. However, we do not know θ_1 or θ_2. We estimate the parameters θ_1 and θ_2 encoded in $\rho_\theta = U(\theta)|\Psi_\downarrow\rangle\langle\Psi_\downarrow|U^\dagger(\theta)$. By doing so, we have an estimate for the expectation value of the position operators $\hat{x}^1$ and $\hat{x}^2$ as seen in Eq. (8).

The parametric model (3) in the rest frame is a classical model in the following sense. First, two parameters are totally uncorrelated since the state vector (6) is also expressed as the tensor product form

$$|\Psi_\downarrow(\theta)\rangle = |\psi_1(\theta_1)\rangle|\psi_2(\theta_2)\rangle|p^3 = 0\rangle|\downarrow\rangle,$$

[1]It is known that a position operator in relativistic quantum mechanics is not uniquely defined (see, for example, Ref. [36] and references therein).

with

$$|\psi_j(\theta_j)\rangle = \int dp^j \varphi_0(p^j) e^{-ip^j\theta_j} |p^j\rangle \quad (j = 1, 2).$$

Second, an optimal measurement to estimate θ_j is the position operator $\hat{x}^j$. Optimal measurements for θ_1 and θ_2 commute and hence we can simultaneously perform the optimal measurement. Third, upon measuring the position operators, the measurement outcomes obey the independent classical Gaussian distributions with the mean (θ_1, θ_2) and their variances $(\kappa^2/2, \kappa^2/2)$. Thus, the optimal unbiased estimator is given by the sample mean.

B. Quantum Fisher information in the rest frame

The SLD $L_j(\theta)$ of the pure state model (3) is calculated, for example, by the method given in [37] as

$$L_j(\theta) = 2\partial_j[|\Psi_\downarrow(\theta)\rangle\langle\Psi_\downarrow(\theta)|], \tag{9}$$

where $\partial_j = \partial/\partial\theta_j$. The SLD Fisher information matrix $J(\theta) = [J_{jk}(\theta)]$ is obtained by the formula in [37] as

$$\begin{aligned} J_{jk} = 4[&\langle\partial_j\Psi_\downarrow(\theta)|\partial_k\Psi_\downarrow(\theta)\rangle \\ &+ \langle\Psi_\downarrow(\theta)|\partial_j\Psi_\downarrow(\theta)\rangle\langle\Psi_\downarrow(\theta)|\partial_k\Psi_\downarrow(\theta)\rangle]. \end{aligned}$$

In the following discussion, we drop θ in the SLD Fisher information matrix because J is independent of θ due to the unitarity of the model. By a straightforward calculation involving the standard Gaussian integrals we have

$$J_{jk} = \frac{2}{\kappa^2}\delta_{jk} \quad (j, k = 1, 2). \tag{10}$$

The inverse of the SLD Fisher information matrix $J^{-1} = [J^{-1}_{jk}]$ is also diagonal:

$$J^{-1}_{jk} = \frac{\kappa^2}{2}\delta_{jk}. \tag{11}$$

The SLD CR inequality is expressed as

$$\mathsf{V} \geqslant J^{-1},$$

where $\mathsf{V} = [\mathsf{V}_{jk}]$ is the mean-square-error matrix. With Eq. (11) we have

$$\mathsf{V}_{11} \geqslant \frac{\kappa^2}{2}, \quad \mathsf{V}_{22} \geqslant \frac{\kappa^2}{2}. \tag{12}$$

The estimation accuracy limit regarding the expectation value of the position operator is proportional to κ^2, which determines the spread of the wave function in the coordinate representation. It is easy to see that J^{-1} approaches the zero matrix as $\kappa \to 0$. In the limit of $\kappa \to 0$, the wave function in the coordinate representation becomes the Dirac delta function. This allows us to estimate the parameter θ without any error.

C. State in a moving frame

We next consider an observer moving along the z axis with respect to the rest frame. A Lorentz transformation Λ from the rest frame to this moving frame is

$$\Lambda = \begin{pmatrix} \cosh\chi & 0 & 0 & -\sinh\chi \\ 0 & 1 & 0 & 0 \\ 0 & 0 & 1 & 0 \\ -\sinh\chi & 0 & 0 & \cosh\chi \end{pmatrix}, \tag{13}$$

$$\cosh\chi = \frac{1}{\sqrt{1-V^2}}, \quad \sinh\chi = \frac{V}{\sqrt{1-V^2}}, \tag{14}$$

where V is the velocity of the observer moving along the z axis. By this Lorentz transformation, the momentum of the particle is transformed as in classical physics. We define the spatial part of the four-momentum $\overrightarrow{\Lambda p}$ as

$$\Lambda p = ((\Lambda p)_0, (\Lambda p)_1, (\Lambda p)_2, (\Lambda p)_3) = ((\Lambda p)_0, \overrightarrow{\Lambda p}). \tag{15}$$

Then $\overrightarrow{\Lambda p}$ is given by

$$\begin{aligned} \overrightarrow{\Lambda p} &= \left(\sum_{\mu=0}^{3}\Lambda^1{}_\mu p^\mu, \sum_{\mu=0}^{3}\Lambda^2{}_\mu p^\mu, \sum_{\mu=0}^{3}\Lambda^3{}_\mu p^\mu\right) \\ &= (p^1, p^2, -p^0\sinh\chi), \end{aligned} \tag{16}$$

where $p^0 = \sqrt{m^2 + |\vec{p}|^2}$ and $|\vec{p}|^2 = (p^1)^2 + (p^2)^2$. The m is a rest mass of the particle (see, for example, Ref. [19]).

For a relativistic spin-1/2 particle, the Lorentz transformation Λ also gives rise to a unitary transformation $U(\Lambda)$ acting on the state vector. This is described by the Wigner rotation [18,19] (see a short summary in Appendix A). The term "rotation" is included because the unitary transformation $U(\Lambda)$ is reduced to the spatial rotation of the Pauli spin. In our model, the state vector in the rest frame is in a spin-down state $|\Psi_\downarrow(\theta)\rangle$. The state vector $|\Psi_\downarrow(\theta)\rangle$ is transformed to $|\Psi^\Lambda(\theta)\rangle$ as

$$|\Psi^\Lambda(\theta)\rangle = U(\Lambda)|\Psi_\downarrow(\theta)\rangle = \sum_{\sigma=\downarrow,\uparrow}\left|\Psi^\Lambda_\sigma(\theta)\right\rangle. \tag{17}$$

We remark here that $|\Psi^\Lambda_\sigma(\theta)\rangle$ $(\sigma = \downarrow, \uparrow)$ are not normalized. It is convenient to express the state vectors $|\Psi^\Lambda_\sigma(\theta)\rangle$ $(\sigma = \downarrow, \uparrow)$ as

$$\left|\Psi^\Lambda_\sigma(\theta)\right\rangle = \left|\psi^\Lambda_\sigma(\theta)\right\rangle|\sigma\rangle.$$

The explicit form of $|\psi^\Lambda_\sigma(\theta)\rangle$ is given by

$$\left|\psi^\Lambda_\sigma(\theta)\right\rangle = \int d^3p\sqrt{\frac{(\Lambda p)^0}{p^0}}F_{\theta,\sigma}(p^1, p^2)\delta(p^3)\left|\Lambda\vec{p}\right\rangle, \tag{18}$$

$$F_{\theta,\downarrow}(p^1, p^2) = \varphi_0(p^1)\varphi_0(p^2)e^{-ip^1\theta_1 - ip^2\theta_2}\cos\frac{\alpha(|\vec{p}|)}{2}, \tag{19}$$

$$F_{\theta,\uparrow}(p^1, p^2) = -\varphi_0(p^1)\varphi_0(p^2)e^{-ip^1\theta_1 - ip^2\theta_2}e^{i\phi(p^1,p^2)}\sin\frac{\alpha(|\vec{p}|)}{2}, \tag{20}$$

$$|\vec{p}| = \sqrt{(p^1)^2 + (p^2)^2},$$

$$e^{i\phi(p^1,p^2)} = \frac{p^1}{|\vec{p}|} + i\frac{p^2}{|\vec{p}|},$$

$$\cos\alpha(|\vec{p}\,|) = \frac{\sqrt{m^2+|\vec{p}\,|^2}+m\cosh\chi}{\sqrt{m^2+|\vec{p}\,|^2}\cosh\chi+m}, \tag{21}$$

$$\sin\alpha(|\vec{p}\,|) = -\frac{|\vec{p}\,|\sinh\chi}{\sqrt{m^2+|\vec{p}\,|^2}\cosh\chi+m}. \tag{22}$$

In the expressions above, m denotes the mass of the spin-1/2 particle in the rest frame.

The Lorentz boost gives a nonzero probability density of spin-up state as shown in Eq. (20). This makes the particle spin rotate and hence is called the Wigner rotation. Detailed derivations of Eqs. (17)–(20) are given in Appendix A.

We remark that the states $|\Psi^\Lambda(\theta)\rangle$ expressed by Eq. (17) are entangled with respect to the momentum and the spin degrees of freedoms. For the observer moving along the z axis, the spin has a component of spin up, which does not exist at the rest frame, i.e., the spin rotates as the observer moves.

III. PARAMETER ESTIMATION: MOVING FRAME

We are now in a position to discuss parameter estimation in the moving frame. Suppose that a moving observer wishes to estimate the parameter θ encoded in the state (17). The system under discussion has two different degrees of freedom. One is continuous describing the wave function and the other is the spin. It is natural to measure the continuous degree of freedom to estimate the parameter as the observer does not know whether they are in a moving frame or not. In this setting, the moving observer does not have access to the spin degree of freedom. Then our parametric model is given by tracing out the spin from the pure state (17).

We also give a short account of other possible cases as a comparison. The first is when the moving observer measures both degrees of freedom. This will be discussed in Sec. III A. The other case is when the spin of the particle is measured only, which will be given in Sec. IV A.

A. Invariance of quantum Fisher information after the Lorentz boost

We first consider the situation where the moving observer measures the whole state (17). The parametric model for this case is defined as

$$\mathcal{M}_{\text{boost}} = \{|\Psi^\Lambda(\theta)\rangle\langle\Psi^\Lambda(\theta)| \mid \theta=(\theta_1,\theta_2)\in\mathbb{R}^2\}. \tag{23}$$

It is clear that this model is unitarily equivalent to the model in the rest frame, since the difference is only given by the unitary transformation $U(\Lambda)$. To phrase it differently, we can regard the model after the Lorentz boost in the different representation. Therefore, the SLD Fisher information matrix is exactly the same as in the rest frame (11). While this is true mathematically, the physical meanings of these two models are different.

Let us further elaborate on the physics of the two models: the one in the rest frame (3) and the other in the moving frame (23). The unitary transformation $U(\Lambda)$ which defines the Wigner rotation is parameter independent; hence, the two parametric models are equivalent. However, the significance of the Lorentz transformation is that $U(\Lambda)$ depends on the velocity V of the moving observer with respect to the rest frame. The resulting state vector after the Lorentz boost (17) indeed depends on V in a nontrivial manner. Furthermore, the wave function in the moving frame is no longer described by the simple Gaussian wave function as given in Eqs. (19) and (20). In particular, the two parameters θ_1 and θ_2 are not described by a tensor product of two independent parametric models as in the rest frame. Nevertheless, we can formally express an optimal measurement for the model after the Lorentz boost by the pair of observables

$$U^\dagger(\Lambda)\hat{x}^j U(\Lambda) \quad (j=1,2),$$

which obviously commute with each other. We will not give further analysis on these observables, but it is evident that experimental implementation of this optimal measurement is much more complex. It may not be feasible as it will depend on the velocity V.

B. Parametric model in the moving frame

We now analyze the parametric model when the moving observer does not measure the spin of the particle. By taking the partial trace over the spin σ, we have

$$\begin{aligned}\rho^\Lambda(\theta) &= \mathrm{tr}_\sigma\, |\Psi^\Lambda(\theta)\rangle\langle\Psi^\Lambda(\theta)| \\ &= \sum_{\sigma=\downarrow,\uparrow} \langle\sigma|\Psi^\Lambda(\theta)\rangle\langle\Psi^\Lambda(\theta)|\sigma\rangle \\ &= \sum_{\sigma=\downarrow,\uparrow} |\psi^\Lambda_\sigma(\theta)\rangle\langle\psi^\Lambda_\sigma(\theta)|.\end{aligned}$$

With this $\rho^\Lambda(\theta)$, we define the parametric model of interest as

$$\mathcal{M}^\Lambda = \{\rho^\Lambda(\theta) \mid \theta=(\theta_1,\theta_2)\in\mathbb{R}^2\}. \tag{24}$$

We note that the resulting model (24) is unitary due to the commutativity of the Lorentz transformation $U(\Lambda)$ and the unitary shift $U(\theta)$.

As noted before, the state vectors $|\psi^\Lambda_\sigma(\theta)\rangle$ are unnormalized. By using the normalized state vector $|\bar{\psi}^\Lambda_\sigma(\theta)\rangle$ defined by

$$|\bar{\psi}^\Lambda_\sigma(\theta)\rangle = \frac{|\psi^\Lambda_\sigma(\theta)\rangle}{\sqrt{\langle\psi^\Lambda_\sigma(\theta)|\psi^\Lambda_\sigma(\theta)\rangle}},$$

we write $\rho^\Lambda(\theta)$ as a convex combination of two pure states $|\bar{\psi}^\Lambda_\downarrow(\theta)\rangle\langle\bar{\psi}^\Lambda_\downarrow(\theta)|$ and $|\bar{\psi}^\Lambda_\uparrow(\theta)\rangle\langle\bar{\psi}^\Lambda_\uparrow(\theta)|$, i.e.,

$$\begin{aligned}\rho^\Lambda(\theta) &= \tfrac{1}{2}(1+\xi)\,|\bar{\psi}^\Lambda_\downarrow(\theta)\rangle\langle\bar{\psi}^\Lambda_\downarrow(\theta)| \\ &\quad + \tfrac{1}{2}(1-\xi)\,|\bar{\psi}^\Lambda_\uparrow(\theta)\rangle\langle\bar{\psi}^\Lambda_\uparrow(\theta)|.\end{aligned}$$

A distinction of this model is that this expression coincides with the eigenvalue decomposition of the state $\rho^\Lambda(\theta)$. In other words, two states $|\bar{\psi}^\Lambda_\uparrow(\theta)\rangle$ and $|\bar{\psi}^\Lambda_\downarrow(\theta)\rangle$ are orthogonal (see Appendix A).

Let us evaluate the inner products $\langle\psi^\Lambda_\sigma(\theta)|\psi^\Lambda_\sigma(\theta)\rangle$ to analyze the amplitudes of each spin state. From Eqs. (18)–(20) the inner products are written as

$$\langle\psi^\Lambda_\downarrow(\theta)|\psi^\Lambda_\downarrow(\theta)\rangle = \tfrac{1}{2}(1+\xi), \tag{25}$$

$$\langle\psi^\Lambda_\uparrow(\theta)|\psi^\Lambda_\uparrow(\theta)\rangle = \tfrac{1}{2}(1-\xi), \tag{26}$$

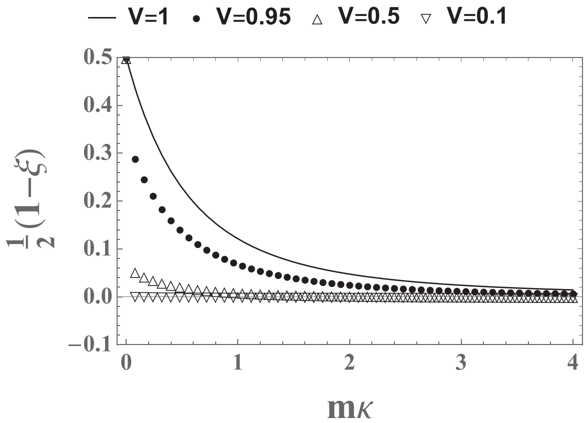

FIG. 1. Numerically calculated $(1-\xi)/2$ as a function of $m\kappa$ at $V=1, 0.95, 0.5$, and 0.1. The set of velocities V is chosen differently to make the distance between the plots more even. The $m\kappa$, ξ, and V are dimensionless in natural units.

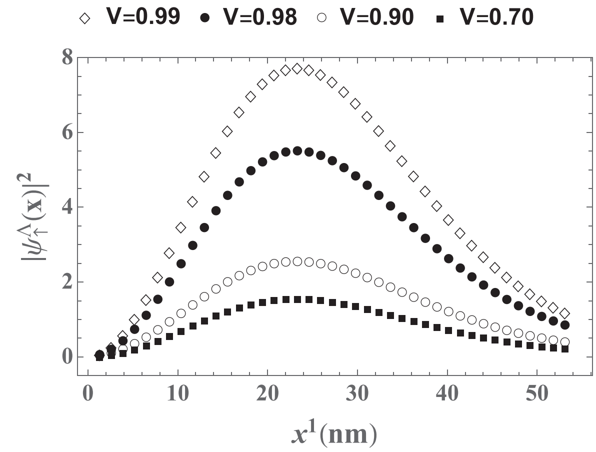

FIG. 2. Numerically calculated probability density $|\psi_\uparrow^\Lambda(x)|^2$ for $\kappa = 0.1\ \mathrm{eV}^{-1}$ as a function of x^1 at $V=0.99, 0.98, 0.9, 0.7$, and 0.1. The distance x^1 is converted to SI units (nm).

where

$$\xi = \int_{-\infty}^{\infty}\int_{-\infty}^{\infty} |\varphi_0(p^1)\varphi_0(p^2)|^2 \cos\alpha(|\vec{p}\,|)dp^1dp^2$$
$$= 2\kappa^2\int_0^\infty dt\, t\, e^{-\kappa^2t^2}\frac{\sqrt{m^2+t^2}\sqrt{1-V^2}+m}{\sqrt{m^2+t^2}+m\sqrt{1-V^2}}. \tag{27}$$

The ξ is an indicator of the spin rotation by the Lorentz boost as seen in Eqs. (25) and (26). As a result, it depends only on the observer's velocity V. The smaller ξ becomes, the larger the amplitude of the spin-up state is. Therefore, the spin rotates.

At any given $m\kappa$, the ξ takes its maximum value 1 at $V=0$, which means no spin rotation. It takes its minimum value ξ_{rel} in the relativistic limit of $V\to 1$, which corresponds to $V\to c$ in the standard unit. An explicit expression of ξ_{rel} is

$$\xi_{\mathrm{rel}} = \sqrt{\pi}m\kappa e^{m^2\kappa^2}\mathrm{erfc}(m\kappa), \tag{28}$$

where $\mathrm{erfc}(x)$ is the complementary error function defined by

$$\mathrm{erfc}(x) = \frac{2}{\sqrt{\pi}}\int_x^\infty dt\, e^{-t^2}.$$

The derivations of Eqs. (25)–(28) are given in Appendix B. The probability for the spin-up state reaches its maximum 1/2 at the limit of $\kappa\to 0$ and at the relativistic limit. Figure 1 shows the probability of the spin-up state $\langle\psi_\uparrow^\Lambda(\theta)|\psi_\uparrow^\Lambda(\theta)\rangle = (1-\xi)/2$ as a function of $m\kappa$ at $V=0.95$, 0.5, and 0.1. The set of velocities V is chosen differently to make the distance between the plots more even. Figure 1 shows its maximum $(1-\xi_{\mathrm{rel}})/2$ as well.

Let us analyze these state vectors in the coordinate representation. We define the wave function of a particle with spin up in the coordinate representation $\psi_\uparrow^\Lambda(x)$ by

$$\psi_\uparrow^\Lambda(x) = \langle x|\bar{\psi}_\uparrow^\Lambda(\theta)\rangle\,|_{\theta=0}.$$

A derivation of its explicit expression is given in Appendix C. Figure 2 shows numerically calculated densities $|\psi_\uparrow^\Lambda(x)|^2$ for $\kappa=0.1$ as a function of the position x^1 for $V=0.99$, 0.98, 0.7, and 0.1. For simplicity, we set $(\theta_1,\theta_2)=(0,0)$ and $x^2, x^3 = 0$. It is worth noting that the peak of the spin-up wave function $\psi_\uparrow^\Lambda(x)$ is no longer at $x^1=\theta_1=0$. To see the dependence of the observer's velocity V on the peak position, we numerically calculate the derivative of $|\psi_\uparrow^\Lambda(x)|^2$. Figure 3 shows the derivative of $|\psi_\uparrow^\Lambda(x)|^2$ as a function of position. In this figure, we set $(\theta_1,\theta_2)=(0,0)$ as well for simplicity. We observe that the faster the observer moves, the farther the peak position moves away from $x^1=\theta_1$. These numerically verified facts indicate that the parametric model (24) is a convex mixture of two pure state models. One is centered at θ and the other is centered at θ plus some amount. If one performs the position measurement, the resulting probability distribution is thus given by a convex mixture of two distributions with different peak locations. This finding naturally leads us to conclude that estimation accuracy gets worse for the moving observer.

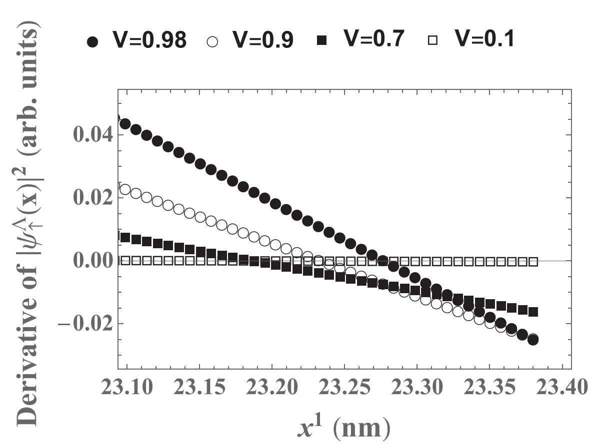

FIG. 3. Numerically calculated derivative of the probability density $|\psi_\uparrow^\Lambda(x)|^2$ as a function of x^1 at $V=0.98, 0.9, 0.7$, and 0.1. The distance x^1 is converted to SI units (nm).

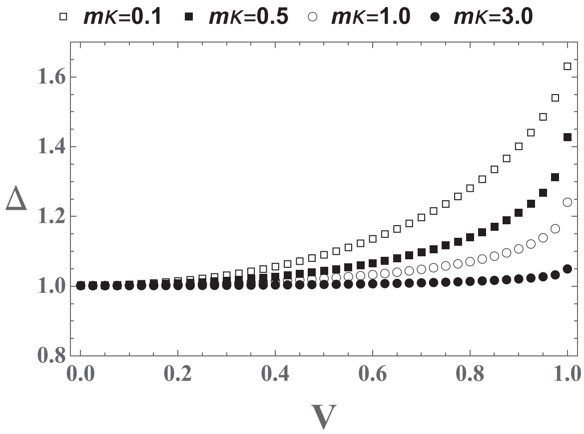

FIG. 4. Numerically calculated ratio $\Delta(V)$ as a function of V, the velocity of the moving observer at $m\kappa = 0.1, 0.5, 1.0$, and 3.0.

C. Quantum Fisher information matrix in the moving frame

The SLD Fisher information matrix $J^{\Lambda} = [J^{\Lambda}{}_{jk}]$ for the model (24) is calculated as

$$J^{\Lambda}{}_{jk} = \frac{2}{\kappa^2}(1 - 2\kappa^2\eta^2)\delta_{jk}, \tag{29}$$

where

$$\eta = -\int_{-\infty}^{\infty}\int_{-\infty}^{\infty} dp^1 dp^2 \frac{(p^1)^2}{|\vec{p}\,|}[\varphi_0(p^1)\varphi_0(p^2)]^2 \sin\alpha(|\vec{p}\,|). \tag{30}$$

A detailed explanation is given in Appendix D. From Eq. (29) we have the SLD CR inequality

$$\mathsf{V}_{11} \geqslant \frac{\kappa^2}{2}\frac{1}{1-2\kappa^2\eta^2}, \quad \mathsf{V}_{22} \geqslant \frac{\kappa^2}{2}\frac{1}{1-2\kappa^2\eta^2}. \tag{31}$$

As given in Appendix E, the denominator in Eq. (31), $1 - 2\kappa^2\eta^2$, is positive and hence the accuracy limits for V_{11} and V_{22} are always finite.

By comparing the SLD CR inequalities for the rest frame [Eqs. (12) and (31)], we see how much estimation accuracy is affected by the Lorentz boost. As an indicator, we take up the ratio of the (1,1) components of $(J^{\Lambda})^{-1}$ and $(J)^{-1}$. We define the ratio $\Delta(V)$ by

$$\Delta(V) = \frac{[(J^{\Lambda})^{-1}]_{11}}{[(J)^{-1}]_{11}} = \frac{1}{1-2\kappa^2\eta^2}. \tag{32}$$

By definition, $\Delta(0) = 1$ for the rest frame. The ratio $\Delta(V)$ quantifies the information loss due to the Lorentz boost. If it is larger, the moving observer can only estimate the parameter less accurately when compared to the rest frame. Figure 4 shows the ratio $\Delta(V)$ as a function the moving observer's velocity V at the different spreads of the wave function $\kappa = 0.1$, 0.5, 1.0, and 3.0. The set of the spreads κ is chosen to make the distance between the plots more even.

From Eqs. (22) and (30), $\kappa\eta$ is expressed as

$$\kappa\eta = V\int_0^{\infty} dt \frac{\kappa'^3 t^3 e^{-\kappa'^2 t^2}}{\sqrt{1+t^2}+\sqrt{1-V^2}},$$

where $\kappa' = m\kappa$. As shown in Appendix E, $\kappa\eta$ is a monotonically decreasing function of $\kappa' = m\kappa$ for any given velocity V. This then implies that $\kappa\eta$ reaches its maximum $\sqrt{\pi}V/4$ at the limit of $\kappa \to 0$. Therefore, for $\Delta(V)$ we obtain the inequality

$$\Delta(V) \leqslant \lim_{\kappa\to 0}\Delta(V) = \frac{1}{1-\frac{\pi}{8}V^2}. \tag{33}$$

D. Quantum Fisher information matrix at the relativistic limit

We will analyze the relativistic limit of our result in detail. First, from Eq. (33), an upper bound for the relativistic limit of the ratio $\Delta(V)$ is given by

$$\Delta(1) \leqslant \frac{1}{1-\frac{\pi}{8}} \simeq 1.647.$$

This shows that the ratio is always finite.

Next we calculate an explicit expression for the relativistic limit of the SLD Fisher information matrix $J^{\mathrm{rel}} = \lim_{V\to 1} J^{\Lambda}$. This is given by

$$J^{\mathrm{rel}}{}_{jk} = \frac{2}{\kappa^2}\left\{1-2\left[\frac{m\kappa}{2}+\frac{\sqrt{\pi}}{4}e^{m^2\kappa^2}(1-2m^2\kappa^2)\mathrm{erfc}(m\kappa)\right]^2\right\} \times \delta_{jk}.$$

It is worth noting that the $(J^{\mathrm{rel}})^{-1}$ is finite even at the relativistic limit of $V \to 1$, which corresponds to that of $V \to c$ in the standard unit. To get further insight into the property of J^{rel}, we consider two different limits in the spread κ of the wave function. We will analyze the small and large κ limit of $(J^{\mathrm{rel}})^{-1}$, as the estimation accuracy limit is quantified by the inverse of J^{rel}.

When the spread is extremely broader $\kappa \gg 1$, with the help of the asymptotic expansion of the complementary error function $\mathrm{erfc}(x)$ (see Appendix E), an approximate expression of $[(J^{\mathrm{rel}})^{-1}]_{11}$ is written as

$$[(J^{\mathrm{rel}})^{-1}]_{11} \simeq [(J)^{-1}]_{11} + \frac{1}{4m^2}.$$

The difference between $[(J^{\mathrm{rel}})^{-1}]_{11}$ and $[(J)^{-1}]_{11}$ is only a constant given by the particle mass.

When the spread is extremely narrower $\kappa \ll 1$, on the other hand, by using the Taylor expansion (Appendix E), we have

$$[(J^{\mathrm{rel}})^{-1}]_{11} \simeq \frac{[(J)^{-1}]_{11}}{1-\frac{\pi}{8}} \simeq 1.647[(J)^{-1}]_{11}.$$

As also seen by Eq. (33), the relativistic effect for the SLD Fisher information matrix is more prominent when the spread is narrower.

IV. DISCUSSION

A. No information left in the spin

We show that if the moving observer does not measure the continuous degree of freedom, the observer cannot estimate the parameter shift in the position by the following reasoning. In other words, no information is left in the spin of the particle. Putting it differently, the Wigner rotation does not transfer the information about the parameter to the spin degree of freedom.

Suppose that the moving observer only measures the spin of the particle. We take the partial trace over the momentum $\vec{p}$

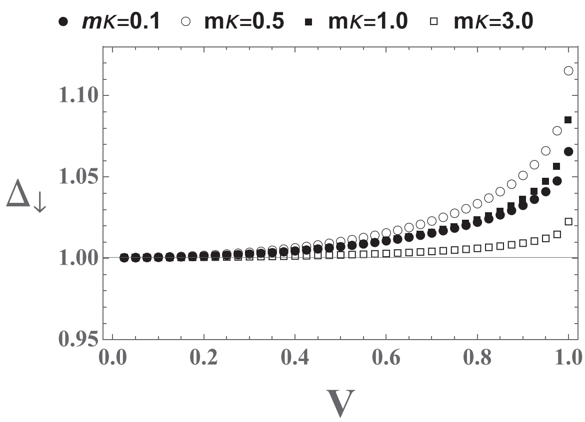

FIG. 5. Numerically calculated ratio $\Delta_{\downarrow}(V)$ as a function of V, the velocity of the moving observer at $m\kappa = 0.1$, 0.5, 1.0, and 3.0. (The scale of the vertical axis is different from that in Fig. 4.) The $m\kappa$ and V are dimensionless in natural units.

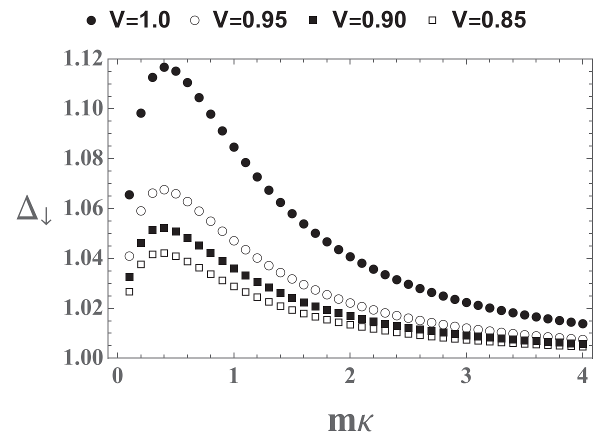

FIG. 6. Numerically calculated ratio $\Delta_{\downarrow}(V)$ as a function of $m\kappa$ for the velocity of the moving observer at $V = 1.0$, 0.95, 0.90, and 0.85.

to obtain the reduced state $\rho^{\Lambda}_{\rm spin}(\theta) = {\rm tr}_{\rm p}\,|\Psi^{\Lambda}(\theta)\rangle\langle\Psi^{\Lambda}(\theta)|$ for this case. The parametric model is then given by

$$\mathcal{M}_{\rm spin} = \{\rho^{\Lambda}_{\rm spin}(\theta)\mid \theta = (\theta_1, \theta_2) \in \mathbb{R}^2\}. \tag{34}$$

From Eqs. (19) and (20) we see that the integrand $F_{\theta,\sigma}(p^1, p^2)F^*_{\theta,\sigma'}(p^1, p^2)$ $(\sigma, \sigma' = \downarrow, \uparrow)$ does not depend on the parameter θ, since the phases cancel each other. Thus, in this situation, we cannot estimate the parameter of the model (34) at all, since the reduced state $\rho^{\Lambda}_{\theta,\rm spin}$ does not depend on the parameter.

B. Information in the down-spin state

Following the preceding section, it is natural to ask where the information about the parameter is located. To examine this, we analyze a hypothetical scenario in which an experimenter accesses the spin-down state only. This is possible, for example, by performing a nondemolition measurement of spin first and then measuring the continuous degree of freedom. In this case, we need to evaluate the SLD Fisher information matrix $J^{\Lambda}_{\downarrow}$ about the pure state model:

$$\{|\bar{\psi}^{\Lambda}_{\downarrow}(\theta)\rangle\langle\bar{\psi}^{\Lambda}_{\downarrow}(\theta)| \mid \theta \in \mathbb{R}^2\}. \tag{35}$$

Using Eqs. (D2) and (D3), we obtain

$$J^{\Lambda}_{\downarrow,\,jk} = \frac{2}{\kappa^2}\delta_{jk}\frac{1 + 2\kappa^2\nu}{1 + \xi}, \tag{36}$$

where ν is defined by

$$\nu = \kappa^2\int_0^{\infty} dt\, t^3\, \frac{\sqrt{m^2+t^2}\sqrt{1-V^2} + m}{\sqrt{m^2+t^2} + m\sqrt{1-V^2}}e^{-\kappa^2 t^2}. \tag{37}$$

With this expression, we define the ratio of the (1,1) components of $(J^{\Lambda}_{\downarrow})^{-1}$ and $(J)^{-1}$ by

$$\Delta_{\downarrow}(V) = \frac{[(J^{\Lambda}_{\downarrow})^{-1}]_{11}}{[(J)^{-1}]_{11}} = \frac{1+\xi}{1 + 2\kappa^2\nu}.$$

Figure 5 shows the ratio $\Delta_{\downarrow}(V)$ as a function the moving observer's velocity V at the different spreads of the wave function $\kappa = 0.1$, 0.5, 1.0, and 3.0. When compared with Fig. 4, we see that the information loss is suppressed, as expected. However, the differences are rather small, i.e., at most a factor of 2. In contrast to Fig. 4, we notably observe a strange behavior for small κ. Figure 5 indicates that relatively small κ (=0.1 in the figure) tends to suppress the information loss more than other values $\kappa = 0.5$ and 1. To examine this effect, we plot $\Delta_{\downarrow}(V)$ as a function of κ for given velocities of the observer $V = 1$, 0.95, 0.9, and 0.8 in Fig. 6. We numerically verify the existence of a peak for each curve. This peak corresponds to the spread of the initial Gaussian state with the maximum information loss. Currently, we do not have a clear physical explanation for this phenomenon.

C. Tradeoff between V and κ

We wish to discuss the role of the spread of the wave function in our result. In the rest frame, κ should be as small as possible to have better estimation accuracy. In Fig. 4 the ratio of estimation accuracies $\Delta(V)$ is shown to be monotonically decreasing in κ for a fixed velocity V. This means that the information loss for a moving observer is reduced by choosing relatively large κ. However, this results in losing estimation accuracy as the broader spread in general enables a less accurate estimation. Therefore, we expect the existence of a tradeoff relation for a moving observer to design the best spread to gain the best information available.

To get further insight into the tradeoff relation, we will analyze the information loss expression (32) when compared with the actual lower bound $[(J^{\Lambda})^{-1}]_{11}$ calculated by (29). Numerically, we verify that $[(J^{\Lambda})^{-1}]_{11}$ is a monotonically increasing function of κ for any fixed V. Thus, a tradeoff relation appears when one attempts to minimize both $[(J^{\Lambda})^{-1}]_{11}$ and $\Delta(V)$ simultaneously. In Fig. 7 we plot the sum of two curves $[(J^{\Lambda})^{-1}]_{11} + \Delta(V)$ to illustrate this tradeoff relation for $V = 0.1$, 0.3, 0.6, 0.8, 0.95, and 1.[2] As seen in this figure,

[2]More generally, we analyze the tradeoff relation with the coefficient to simplify the analysis of $(J^{\Lambda})^{-1}$. We make $(J^{\Lambda})^{-1}$ dimensionless by the coefficient.

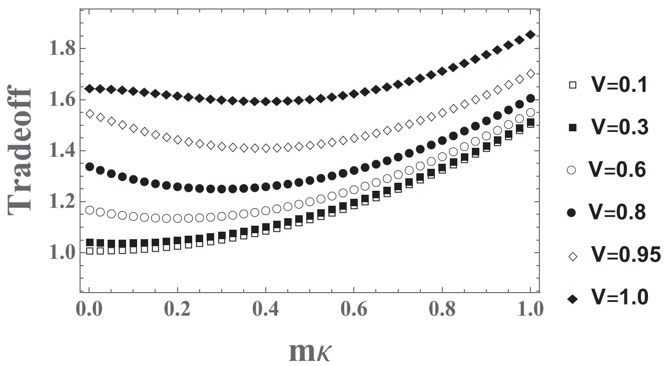

FIG. 7. Numerically calculated the sum of $[(J^{\Lambda})^{-1}]_{11} + \Delta(V)$ to illustrate this tradeoff relation for $V = 0.1$, 0.3, 0.6, 0.8, 0.95, and 1.0.

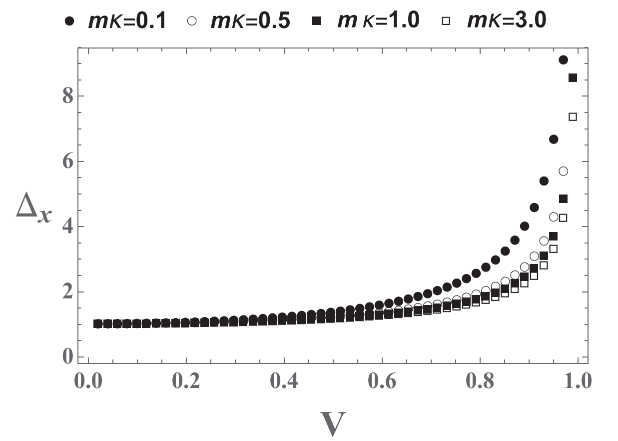

FIG. 8. Numerically calculated ratio $\Delta_x(V)$ as a function of V, the velocity of the moving observer at $\kappa = 0.1$, 0.5, 1.0, and 3.0. (The scale of the vertical axis is different from that in Fig. 4.)

the optimal choice κ_* for the spread becomes larger for larger V. As a rough estimate, we find $\kappa_* \simeq V/2$.

D. Possible experimental realization

In this section we discuss a possible experimental realization of our result. To this end, we consider estimation of one of two parameters, whereas the other is treated as the nuisance parameter [38]. In the following, we treat θ_1 as the parameter of interest to be estimated.

In this setting, the ultimate precision limit upon estimating θ_1 is given by the (1,1) component of the inverse of the SLD Fisher information matrix. Hence, $[(J^{\Lambda})^{-1}]_{11}$ has an operational meaning. The optimal measurement to attain this bound is given by the spectral decomposition of the SLD operator, since the SLD Fisher information is diagonal in our model [38]. This optimal measurement, however, depends on the velocity of the observer in a complex manner, and this is not easy to perform in a laboratory. We then consider alternative setting as follows.

Instead of performing the above optimal measurement, suppose the observer chooses the standard position measurement. We quantify the amount of information extracted for this position measurement by the quantum covariance matrix V_{cov}. We then compare V_{cov} and the maximal information set by J^{Λ}. In Appendix F we give a calculation of V_x and the result is

$$\mathsf{V}_{\text{cov}} = \frac{\kappa^2}{2}\frac{1}{\sqrt{1-V^2}}\left[1 + \frac{V^2}{2}\mu_1 + (1-\sqrt{1-V^2})\mu_2\right]I,$$

where μ_1 and μ_2 are defined by

$$\mu_1 = \int_0^\infty dt\,\frac{t}{(1+t^2)(\sqrt{1+t^2}+\sqrt{1-V^2})^2}e^{-\kappa'^2 t^2},$$

$$\mu_2 = \int_0^\infty dt\,\frac{1}{t}\frac{\sqrt{1+t^2}-1}{\sqrt{1+t^2}+\sqrt{1-V^2}}e^{-\kappa'^2 t^2}.$$

The information loss, which a laboratory can access, is defined by

$$\Delta_x(V) = \frac{\mathsf{V}_{\text{cov},11}}{[(J)^{-1}]_{11}}. \tag{38}$$

In Fig. 8 we plot the ratio $\Delta_x(V)$ as a function of the moving observer's velocity V at the different spreads of the wave function $\kappa = 0.1, 0.5, 1.0$, and 3.0. The ratio Δ_x diverges in the relativistic limit of $V \to 1$ because the relativistic factor $1/\sqrt{1-V^2}$ diverges. The μ_1 and μ_2 are finite even in the relativistic limit. This figure should be compared with the theoretical limit as shown in Fig. 4. Clearly, we have more information loss by performing the standard position measurement, since this is not an optimal measurement. However, this figure clearly shows that the information loss due to relativity can be accessed in an actual experiment. It also shows that the relativistic effect is more visible for narrow spreads in general.

E. Effect of Wigner rotation

We now discuss the effect of the Wigner rotation on estimation accuracy in our model. As we have seen in Sec. III B, the Wigner rotation gives the amplitudes of both the spin-up and spin-down states. When a moving observer measures the momentum only, the observer ends up seeing the effect of the Wigner rotation as the mixture of two different pure states (18). This then gives rise to information loss, as the measurement of the momentum only is not complete. This information loss for the moving observer is of course expected. This is because the effect of the Wigner rotation followed by the partial trace is a completely positive and trace-preserving map. Therefore, the SLD Fisher information should decrease by the monotonicity of the quantum Fisher information. One of the nontrivial findings of our paper is the explicit formula for this information loss as a function of the velocity of the observer.

We further elaborate on the parametric model for a moving observer. The wave function of the spin-up state $\psi^{\Lambda}_{\uparrow}(x)$, which does not exist in the rest frame, appears due to the Wigner rotation. The peak of the probability density $|\psi^{\Lambda}_{\uparrow}(x)|^2$ no longer exists at $(x^1, x^2) = (\theta_1, \theta_2)$. Our numerical calculation indicates that it moves farther away from the point (θ_1, θ_2) as the velocity of the observer V increases (Figs. 2 and 3). Because of this extra peak, estimation of the expectation values of the position operators is disturbed; therefore, the SLD CR bound increases. The ratio of the upper bound of the moving frame to the rest frame is given by $(1-2\kappa^2\eta^2)^{-1}$, where η is explicitly expressed as the integral form.

The relativistic limit of the SLD Fisher information is also a rather unexpected result. In Fig. 2 we numerically evaluated the relativistic behaviors of the density for the spin-up state. As the velocity approaches the speed of light, we observe that the height of the peak increases rapidly. This implies that the peak diverges in the relativistic limit. This is partially because the Lorentz transformation (14) does not have a well-defined limit. However, the SLD Fisher information matrix remains finite even in this limit, which is calculated by the derivatives of the state. Thus, the SLD CR bound does not diverge even at the relativistic limit.

Finally, we briefly discuss the achievability of the SLD CR bounds. We show that the SLD CR bound in the rest frame is achievable. When an observer is moving and does not measure the spin, the derived SLD CR bound (31) is not achievable. This is shown by checking the weak commutativity condition [39,40]. In Appendix D we calculate this condition and find that $\mathrm{tr}(\rho_\theta^\Lambda[L_1^\Lambda(\theta), L_2^\Lambda(\theta)]) = 8i\xi\eta^2 \neq 0$. Therefore, the SLD CR bound in the moving frame is not achievable even asymptotically. A further investigation of asymptotically and nonasymptotically achievable bounds is left for future work.

V. CONCLUSION

We obtained the accuracy limit for estimating the expectation value of the position of a relativistic particle for an observer moving in one direction at a constant velocity. We evaluated estimation accuracy of the position by the SLD CR bound. Estimation accuracy is degraded by increasing the observer's velocity. We saw that this is because the spin-up state appears in the moving frame while the spin-down state exists in the rest frame. Furthermore, it stays finite even at the relativistic limit. However, since the Wigner rotation can be expressed as a rotation matrix that acts on a state vector, we expect that any divergent behavior will not arise from the result of applying the Wigner rotation to a state vector with a finite spread. Since we showed that the SLD CR bound is not achievable, it is important to have an achievable bound for future work.

ACKNOWLEDGMENTS

The work was partly supported by JSPS KAKENHI Grant No. JP21K11749. We would like to thank Dr. P. Caban for useful comments on the manuscript. We also sincerely thank the anonymous reviewer for constructive comments and valuable suggestions to improve this paper.

APPENDIX A: WIGNER ROTATION

For a massive particle with spin 1/2, we have the relation [18,19]

$$U(\Lambda)\,|p,\sigma\rangle = \sqrt{\frac{(\Lambda p)^0}{p^0}} \sum_{\sigma'=\downarrow,\uparrow} D^{(1/2)}_{\sigma',\sigma}(W(\Lambda,p))\,|\Lambda p,\sigma\rangle\,, \tag{A1}$$

where $W(\Lambda,p) = L^{-1}(\Lambda p)\Lambda L(p)$ and $D^{(1/2)}$ is the spin-1/2 representation of a three-dimensional rotational group. Wigner rotation is an alternative to representing the Lorentz transformation as a unitary transformation described by the Poincaré group on the Dirac spinor. Wigner rotation uses a little group, which was well exposed by Weinberg and Halpern [Eq. (2.5.23) on p. 68 in Ref. [18]] and Halpern [Eq. (37) on p. 67 in Ref. [19]]. This choice is more convenient since we can restrict the Dirac spinor to two components. The mathematical link between the Lorentz group described by $L(p)$ and the 2×2 representation is given by the formula (A1). The essential part is calculating the spatial part of $W(\Lambda,p)$ and then converting it to a rotation on the Pauli spin (see, for example, Ref. [41]). Here the rotational group is evaluated by the spatial part of the matrix $W(\Lambda,p)$. The Lorentz boost $L(p) = [L^i{}_j(p)]$ is chosen as in [18],

$$\begin{aligned} L^i{}_j(p) &= \delta_{ij} + \frac{(\sqrt{m^2+|\vec{p}\,|^2}-m)p^ip^j}{m|\vec{p}\,|^2},\\ L^i{}_0(p) &= \frac{p^i}{m},\\ L^0{}_0(p) &= \frac{\sqrt{m^2+|\vec{p}\,|^2}}{m}. \end{aligned}$$

A direct calculation for our setting $\vec{p} = (p^1, p^2, 0)$ gives the explicit representation of the matrix $W(\Lambda,p)$:

$$\begin{aligned} &[W(\Lambda,p)]^0{}_0 = 1,\\ &[W(\Lambda,p)]^1{}_0 = [W(\Lambda,p)]^0{}_1 = 0,\\ &[W(\Lambda,p)]^2{}_0 = [W(\Lambda,p)]^0{}_2 = 0,\\ &[W(\Lambda,p)]^3{}_0 = [W(\Lambda,p)]^0{}_3 = 0, \end{aligned}$$

$$[W(\Lambda,p)]^1{}_1 = [W(\Lambda,p)]^2{}_2 = \frac{p^0[m(p^1)^2 + p^0(p^2)^2]\sinh^2\chi + |\vec{p}\,|^2[(p^1)^2\cosh\chi + (p^2)^2]}{|\vec{p}\,|^2[(p^0)^2\sinh^2\chi + |\vec{p}\,|^2]},$$

$$[W(\Lambda,p)]^2{}_1 = [W(\Lambda,p)]^1{}_2 = -\frac{p^1p^2(\cosh\chi-1)(p^0-m)}{|\vec{p}\,|^2(p^0\cosh\chi+m)},\quad [W(\Lambda,p)]^3{}_1 = -[W(\Lambda,p)]^1{}_3 = -\frac{p^1\sinh\chi}{p^0\cosh\chi+m},$$

$$[W(\Lambda,p)]^3{}_2 = -[W(\Lambda,p)]^2{}_3 = -\frac{p^2\sinh\chi}{p^0\cosh\chi+m},\quad [W(\Lambda,p)]^3{}_3 = \frac{p^0+m\cosh\chi}{m+p^0\cosh\chi}.$$

A 3×3 real matrix $[R(\Lambda, p)]_{jk}$ is defined by the spatial part of $W(\Lambda, p)$ as

$$[R(\Lambda, p)]_{jk} = [W(\Lambda, p)]^j{}_k \quad (j, k = 1, 2, 3).$$

This is a real rotation matrix acting on the three-dimensional vector space. We next decompose the rotation matrix $R(\Lambda, p)$ with the Euler angles. A straightforward calculation shows that we need only two Euler angles in this case. The matrices $R_2(\alpha)$ and $R_3(\phi)$ express a rotation by angles α and ϕ around the 2- and the 3-axis, respectively [41], i.e.,

$$R(\Lambda, p) = R_3(-\phi)R_2(\alpha)R_3(\phi), \tag{A2}$$

where

$$R_2(\alpha) = \begin{pmatrix} \cos\alpha & 0 & -\sin\alpha \\ 0 & 1 & 0 \\ \sin\alpha & 0 & \cos\alpha \end{pmatrix},$$

$$R_3(\phi) = \begin{pmatrix} \cos\phi & -\sin\phi & 0 \\ \sin\phi & \cos\phi & 0 \\ 0 & 0 & 1 \end{pmatrix}.$$

As we have the Euler rotation representation (A2), we obtain the 2×2 matrix representation of the rotation for the spin-1/2 particle [41] $D^{(1/2)}(W(\Lambda, p))$ as

$$\begin{aligned} D^{(1/2)}(W(\Lambda, p)) &= e^{i\phi(\sigma_3/2)}e^{-i\alpha(\sigma_2/2)}e^{-i\phi(\sigma_3/2)} \\ &= \begin{pmatrix} \cos\frac{\alpha}{2} & -e^{i\phi}\sin\frac{\alpha}{2} \\ e^{-i\phi}\sin\frac{\alpha}{2} & \cos\frac{\alpha}{2} \end{pmatrix}. \end{aligned} \tag{A3}$$

By substituting the expression of $D^{(1/2)}(W(\Lambda, p))$ in (A1), we obtain Eqs. (17)–(20).

APPENDIX B: INNER PRODUCT $\langle \psi^\Lambda_\sigma(\theta)|\psi^\Lambda_{\sigma'}(\theta)\rangle$

From Eq. (18), $\langle \psi^\Lambda_\sigma(\theta)|\psi^\Lambda_{\sigma'}(\theta)\rangle$ is calculated as

$$\begin{aligned} \left\langle \psi^\Lambda_\sigma(\theta)\middle|\psi^\Lambda_{\sigma'}(\theta)\right\rangle &= \int d^3p \int d^3p' \sqrt{\frac{(\Lambda p)^0}{p^0}} F^*_{\theta,\sigma}(p^1, p^2)\delta(p^3) \\ &\quad \times \sqrt{\frac{(\Lambda p')^0}{p'^0}} F_{\theta,\sigma'}(p'^1, p'^2)\delta(p'^3)\,\langle \Lambda\vec{p}\,|\Lambda\vec{p}'\rangle \\ &= \iint dp^1dp^2 F^*_{\theta,\sigma}(p^1, p^2)F_{\theta,\sigma'}(p^1, p^2). \end{aligned}$$

Here we use the relation [18]

$$\langle \overrightarrow{\Lambda p}|\overrightarrow{\Lambda p'}\rangle = \frac{p^0}{(\Lambda p)^0}\,\langle \vec{p}\,|\vec{p}'\rangle = \frac{p^0}{(\Lambda p)^0}\delta(\vec{p} - \vec{p}').$$

For different spin states ($\sigma \neq \sigma'$) this integral vanishes, since it is expressed as an odd function of p^1 and p^2. We thus need to evaluate the case $\sigma = \sigma'$. Using Eqs. (19)–(22), we obtain Eqs. (25), (26), and (28), i.e.,

$$\langle \psi^\Lambda_\downarrow(\theta)|\psi^\Lambda_\downarrow(\theta)\rangle = \tfrac{1}{2}(1+\xi),$$
$$\langle \psi^\Lambda_\uparrow(\theta)|\psi^\Lambda_\uparrow(\theta)\rangle = \tfrac{1}{2}(1-\xi),$$

where

$$\xi = 2\kappa^2\int_0^\infty dt\, t\, e^{-\kappa^2t^2}\frac{\sqrt{m^2+t^2}\sqrt{1-V^2}+m}{\sqrt{m^2+t^2}+m\sqrt{1-V^2}}.$$

From the equation above, we see that ξ is a monotonically decreasing function of $\sqrt{1-V^2}$. Therefore, ξ is a monotonically increasing function of V. When $V = 1$, ξ takes its minimum $\xi_{\rm rel}$, which is evaluated as

$$\xi_{\rm rel} = 2\kappa^2\int_0^\infty \frac{t\,e^{-\kappa^2t^2}}{\sqrt{m^2+t^2}}dt = \sqrt{\pi}m\kappa e^{m^2\kappa^2}\mathrm{erfc}(m\kappa).$$

By performing the standard Gaussian integration, we see that $\xi = 1$ when $V = 0$.

APPENDIX C: PROBABILITY DENSITY OF A SPIN-1/2 PARTICLE: X REPRESENTATION

We define the wave function of a particle with up spin in coordinate representation $\psi^\Lambda_\uparrow(x)$ by

$$\psi^\Lambda_\uparrow(x) = \langle x|\bar{\psi}^\Lambda_\uparrow(\theta)\rangle\,|_{\theta=0}.$$

From Eqs. (20) and (26), the wave function $\psi^\Lambda_\uparrow(x)$ is given by

$$\begin{aligned} \psi^\Lambda_\uparrow(x) &= -\sqrt{\frac{2}{1-\xi}}\int d^3p\sqrt{\frac{(\Lambda p)^0}{p^0}}\varphi_0(p^1, p^2)e^{i\phi(p^1,p^2)} \\ &\quad \times \sin\frac{\alpha(p)}{2}\delta(p^3)\,\langle x|\Lambda p\rangle\,, \end{aligned}$$

where $\varphi_0(p^1, p^2) = \varphi_0(p^1)\varphi_0(p^2)$. By a direct calculation, we have the wave function $\psi^\Lambda_\uparrow(x)$ as

$$\begin{aligned} \psi^\Lambda_\uparrow(x) &= -\sqrt{\frac{2}{1-\xi}}\frac{\kappa}{(2\pi)^2}\sqrt{\cosh\chi} \\ &\quad \times \int dp^1dp^2e^{-\kappa^2[(p^1)^2+(p^2)^2]+i\phi(p^1,p^2)} \\ &\quad \times \sin\frac{\alpha(p)}{2}e^{-ip^1x^1-ip^2x^2-i\sqrt{(p^1)^2+(p^2)^2+m^2}\sinh\chi x^3}. \end{aligned}$$

APPENDIX D: SLD AND SLD FISHER INFORMATION MATRIX

1. SLD Fisher information matrix

The state we are considering $\rho^\Lambda(\theta)$ is written as

$$\begin{aligned} \rho^\Lambda(\theta) &= \tfrac{1}{2}(1+\xi)\,|\bar{\psi}^\Lambda_\downarrow(\theta)\rangle\,\langle\bar{\psi}^\Lambda_\downarrow(\theta)| \\ &\quad + \tfrac{1}{2}(1-\xi)\,|\bar{\psi}^\Lambda_\uparrow(\theta)\rangle\,\langle\bar{\psi}^\Lambda_\uparrow(\theta)|\,. \end{aligned}$$

For multiparameter models, the SLD Fisher information matrix J^Λ for the state $\rho^\Lambda(\theta)$ which is nonfull rank is calculated as

$$\begin{aligned} J^\Lambda{}_{jk} &= 2(1+\xi)[\mathrm{Re}\,\langle\partial_j\bar{\psi}^\Lambda_\downarrow(\theta)|\partial_k\bar{\psi}^\Lambda_\downarrow(\theta)\rangle \\ &\quad - \langle\partial_j\bar{\psi}^\Lambda_\downarrow(\theta)|\bar{\psi}^\Lambda_\downarrow(\theta)\rangle\,\langle\bar{\psi}^\Lambda_\downarrow(\theta)|\partial_k\bar{\psi}^\Lambda_\downarrow(\theta)\rangle] \\ &\quad + 2(1-\xi)[\mathrm{Re}\,\langle\partial_j\bar{\psi}^\Lambda_\uparrow(\theta)|\partial_k\bar{\psi}^\Lambda_\uparrow(\theta)\rangle \\ &\quad - \langle\partial_j\bar{\psi}^\Lambda_\uparrow(\theta)|\bar{\psi}^\Lambda_\uparrow(\theta)\rangle\,\langle\bar{\psi}^\Lambda_\uparrow(\theta)|\partial_k\bar{\psi}^\Lambda_\uparrow(\theta)\rangle] \\ &\quad - 4(1-\xi)(1+\xi) \\ &\quad \times \mathrm{Re}[\langle\bar{\psi}^\Lambda_\uparrow(\theta)|\partial_j\bar{\psi}^\Lambda_\downarrow(\theta)\rangle^*\,\langle\bar{\psi}^\Lambda_\uparrow(\theta)|\partial_k\bar{\psi}^\Lambda_\downarrow(\theta)\rangle]. \end{aligned} \tag{D1}$$

Regarding the calculation, see, for example, [42]. Below, the terms appearing in the second and fourth terms of Eq. (D1) vanish because their integrands are an odd function of p^j, i.e.,

$$\langle \partial_j \bar{\psi}^{\Lambda}_{\sigma}(\theta) | \bar{\psi}^{\Lambda}_{\sigma}(\theta) \rangle = 0 \quad (\sigma = \downarrow, \uparrow). \tag{D2}$$

From Eqs. (18)–(20), the inner products $\langle \partial_j \bar{\psi}^{\Lambda}_{\sigma}(\theta) | \partial_j \bar{\psi}^{\Lambda}_{\sigma}(\theta) \rangle$ $(j, k = 1, 2)$ are obtained as

$$\langle \partial_j \bar{\psi}^{\Lambda}_{\downarrow}(\theta) | \partial_k \bar{\psi}^{\Lambda}_{\downarrow}(\theta) \rangle = \delta_{jk} \frac{(2\kappa^2)^{-1} + \nu}{1+\xi},$$
$$\langle \partial_j \bar{\psi}^{\Lambda}_{\uparrow}(\theta) | \partial_k \bar{\psi}^{\Lambda}_{\uparrow}(\theta) \rangle = \delta_{jk} \frac{(2\kappa^2)^{-1} - \nu}{1-\xi}, \tag{D3}$$

where

$$\nu = \int_{-\infty}^{\infty} \int_{-\infty}^{\infty} dp^1 dp^2 (p^1)^2 [\varphi_0(p^1, p^2)]^2 \cos\alpha(|\vec{p}\,|).$$

Using Eq. (21), it is also written as

$$\nu = \kappa^2 \int_0^{\infty} dt\, t^3 \frac{\sqrt{m^2+t^2}\sqrt{1-V^2} + m}{\sqrt{m^2+t^2} + m\sqrt{1-V^2}} e^{-\kappa^2 t^2}. \tag{D4}$$

We also use Eq. (2)

$$\varphi_0(p^j) = \frac{\kappa^{1/2}}{\pi^{1/4}} e^{-\kappa^2 (p^j)^2/2}$$

and

$$\iint dp^1 dp^2 (p^1)^2 [\varphi_0(p^1, p^2)]^2 = \frac{1}{2\kappa^2}.$$

As for $\langle \partial_j \bar{\psi}^{\Lambda}_{\downarrow}(\theta) | \bar{\psi}^{\Lambda}_{\uparrow}(\theta) \rangle$ $(j = 1, 2)$, a direct calculation gives

$$\langle \partial_1 \bar{\psi}^{\Lambda}_{\downarrow}(\theta) | \bar{\psi}^{\Lambda}_{\uparrow}(\theta) \rangle = -\frac{i\eta}{\sqrt{(1+\xi)(1-\xi)}},$$
$$\langle \partial_2 \bar{\psi}^{\Lambda}_{\downarrow}(\theta) | \bar{\psi}^{\Lambda}_{\uparrow}(\theta) \rangle = -\frac{\eta}{\sqrt{(1+\xi)(1-\xi)}},$$

where

$$\eta = -\int_{-\infty}^{\infty} \int_{-\infty}^{\infty} dp^1 dp^2 \frac{(p^j)^2}{|\vec{p}\,|} [\varphi_0(p^1, p^2)]^2 \sin\alpha(|\vec{p}\,|). \tag{D5}$$

The SLD Fisher information matrix J^{Λ} is expressed as

$$J^{\Lambda} = 2(\kappa^{-2} - 2\eta^2) \begin{pmatrix} 1 & 0 \\ 0 & 1 \end{pmatrix}.$$

It turns out the ν has no effect on the SLD Fisher information.

2. SLD

The SLDs $L^{\Lambda}(\theta)_j$ $(j = 1, 2)$ are expressed as

$$\begin{aligned} L^{\Lambda}{}_{1}(\theta) = {} & \frac{4}{1+\xi} \partial_1 [|\bar{\psi}^{\Lambda}_{\downarrow}(\theta)\rangle \langle \bar{\psi}^{\Lambda}_{\downarrow}(\theta)|] \\ & + \frac{4}{1-\xi} \partial_1 [|\bar{\psi}^{\Lambda}_{\uparrow}(\theta)\rangle \langle \bar{\psi}^{\Lambda}_{\uparrow}(\theta)|] \\ & + 2i\xi\eta [|\bar{\psi}^{\Lambda}_{\downarrow}(\theta)\rangle \langle \bar{\psi}^{\Lambda}_{\uparrow}(\theta)| - |\bar{\psi}^{\Lambda}_{\uparrow}(\theta)\rangle \langle \bar{\psi}^{\Lambda}_{\downarrow}(\theta)|], \end{aligned}$$

$$\begin{aligned} L^{\Lambda}{}_{2}(\theta) = {} & \frac{4}{1+\xi} \partial_2 [|\bar{\psi}^{\Lambda}_{\downarrow}(\theta)\rangle \langle \bar{\psi}^{\Lambda}_{\downarrow}(\theta)|] \\ & + \frac{4}{1-\xi} \partial_2 [|\bar{\psi}^{\Lambda}_{\uparrow}(\theta)\rangle \langle \bar{\psi}^{\Lambda}_{\uparrow}(\theta)|] \\ & + 2\xi\eta [|\bar{\psi}^{\Lambda}_{\downarrow}(\theta)\rangle \langle \bar{\psi}^{\Lambda}_{\uparrow}(\theta)| - |\bar{\psi}^{\Lambda}_{\uparrow}(\theta)\rangle \langle \bar{\psi}^{\Lambda}_{\downarrow}(\theta)|]. \end{aligned}$$

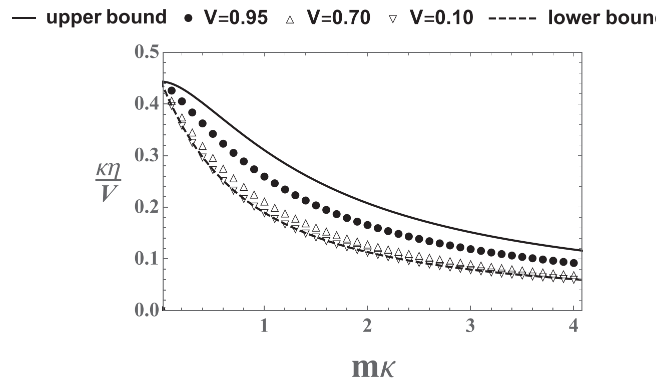

FIG. 9. Plot of $\kappa\eta/V$ as a function of $m\kappa$ at $V = 0.95$, 0.7, and 0.1.

By using these, we can show that $L^{\Lambda}{}_{1}(\theta)$ and $L^{\Lambda}{}_{2}(\theta)$ do not commute, i.e., $[L^{\Lambda}{}_{1}(\theta), L^{\Lambda}{}_{2}(\theta)] \neq 0$.

Furthermore, by a direct calculation, we can evaluate the weak commutativity condition as

$$\mathrm{tr}\{\rho^{\Lambda}_{\theta} [L^{\Lambda}{}_{1}(\theta), L^{\Lambda}{}_{2}(\theta)]\} = 8i\xi\eta^2 \neq 0.$$

This shows that the SLD CR bound is not achievable even in the asymptotic setting.

APPENDIX E: MAXIMUM AND MINIMUM OF $\kappa\eta$

From Eq. (30), $\kappa\eta$ is expressed as

$$\kappa\eta = V \int_0^{\infty} dt \frac{\kappa'^3 t^3 e^{-\kappa'^2 t^2}}{\sqrt{1+t^2} + \sqrt{1-V^2}}.$$

By the velocity dependence of the integrand, we have an upper bound with $V = 1$ and a lower bound with $V = 0$. We obtain the following inequality for $\kappa\eta$:

$$V \int_0^{\infty} dt \frac{\kappa'^3 t^3 e^{-\kappa'^2 t^2}}{\sqrt{1+t^2} + 1} \leqslant k\eta \leqslant V \int_0^{\infty} dt \frac{\kappa'^3 t^3 e^{-\kappa'^2 t^2}}{\sqrt{1+t^2}}.$$

These integrations are explicitly written as

$$\int_0^{\infty} dt \frac{\kappa'^3 t^3 e^{-\kappa'^2 t^2}}{\sqrt{1+t^2} + 1} = \frac{\sqrt{\pi}}{4} e^{\kappa'^2} \mathrm{erfc}(\kappa'), \tag{E1}$$

$$\int_0^{\infty} dt \frac{\kappa'^3 t^3 e^{-\kappa'^2 t^2}}{\sqrt{1+t^2}} = \frac{\kappa'}{2} + \frac{\sqrt{\pi}}{4} e^{\kappa'^2} (1 - 2\kappa'^2) \mathrm{erfc}(\kappa'). \tag{E2}$$

The right-hand sides of Eqs. (E1) and (E2) are monotonically decreasing functions of κ' or $m\kappa$. Their maxima at the limit of $\kappa \to 0$ for both are $\sqrt{\pi}V/4$, i.e., $\kappa\eta < \sqrt{\pi}V/4$ for any $\kappa > 0$. Figure 9 shows numerically calculated $|\kappa\eta|/V$ together with the upper and lower bounds.

By using the asymptotic expansion of the complimentary error function $\mathrm{erfc}(x)$,

$$\mathrm{erfc}(x) = \frac{e^{-x^2}}{\sqrt{\pi}x} \sum_{n=0}^{\infty} (-1)^n \frac{(2n-1)!!}{2^n x^{2n}},$$

for $\kappa' \gg 1$, we have

$$\int_0^\infty dt \frac{\kappa'^3 t^3 e^{-\kappa'^2 t^2}}{\sqrt{1+t^2}+1} \simeq \frac{1}{4\kappa'},$$
$$\int_0^\infty dt \frac{\kappa'^3 t^3 e^{-\kappa'^2 t^2}}{\sqrt{1+t^2}} \simeq \frac{1}{2\kappa'}.$$

Then $\Delta(V)$ is approximately expressed as

$$1+\frac{V^2}{8\kappa'^2} \leqslant \Delta(V) \leqslant 1+\frac{V^2}{2\kappa'^2}.$$

For $\kappa' \ll 1$, by the Taylor expansion we have

$$\frac{1}{1-\frac{\pi V^2}{8}}\left(1-\frac{\pi}{4}\frac{V^4\kappa'^2}{1-\frac{\pi V^2}{8}}\right) \leqslant \Delta(V) \leqslant \frac{1}{1-\frac{\pi V^2}{8}}\left(1-\frac{\sqrt{\pi}}{2}\frac{V^2\kappa'}{1-\frac{\pi V^2}{8}}\right).$$

APPENDIX F: CALCULATION OF THE QUANTUM COVARIANCE V_x

Upon performing the position measurement about the x axis, we have a continuous probability density function

$$\begin{aligned} p_\theta(x) &= \langle x|\,\rho^\Lambda(\theta)\,|x\rangle \\ &= \tfrac{1}{2}(1+\xi)|\,\langle x|\bar{\psi}^\Lambda_\downarrow(\theta)\rangle\,|^2 + \tfrac{1}{2}(1-\xi)|\,\langle x|\bar{\psi}^\Lambda_\uparrow(\theta)\rangle\,|^2. \end{aligned}$$

The mean-square-error matrix is then evaluated by the usual integration over $x=(x^1,x^2)$. Instead, we evaluate the quantum covariance $\mathsf{V}_{\rm cov}$,

$$\begin{aligned} \mathsf{V}_{\rm cov} &= [\mathsf{V}_{{\rm cov},jk}], \\ \mathsf{V}_{{\rm cov},jk} &= {\rm tr}[\rho^\Lambda(\theta)\hat{x}^j\hat{x}^k] - {\rm tr}[\rho^\Lambda(\theta)\hat{x}^j]{\rm tr}[\rho^\Lambda(\theta)\hat{x}^k]. \end{aligned}$$

In the following, $\mathsf{V}_{{\rm cov},jk}$ is evaluated by using a p representation in which $\hat{x}^j$ are represented by partial derivatives about p^j. First, we note that the expectation value of $\hat{x}^j$ is simply calculated as θ_j. To see this, we evaluate

$$\begin{aligned} \sum_\sigma \langle \psi^\Lambda_\sigma(\theta)|\hat{x}^j|\psi^\Lambda_\sigma(\theta)\rangle &= \sum_\sigma \langle \psi^\Lambda_\sigma(0)|(\hat{x}^j+\theta_j)|\psi^\Lambda_\sigma(0)\rangle \\ &= \sum_\sigma \langle \psi^\Lambda_\sigma(0)|\hat{x}^j|\psi^\Lambda_\sigma(0)\rangle + \theta_j, \end{aligned}$$

where the first term vanishes for the following reasons. In the case of a spin-down state, $\langle\psi^\Lambda_\downarrow(0)|\hat{x}^j|\psi^\Lambda_\downarrow(0)\rangle$ is expressed as

$$\begin{aligned} &\langle\psi^\Lambda_\downarrow(0)|\hat{x}^j|\psi^\Lambda_\downarrow(0)\rangle \\ &= \cosh\chi \iint dp^1dp^2 F^*_{0,\downarrow}(p^1,p^2)\hat{x}^j F_{0,\downarrow}(p^1,p^2). \end{aligned}$$

The term $|F_{0,\downarrow}(p^1,p^2)|^2$ is an even function of p^1 and p^2. Moreover, the partial derivatives of it are odd functions. On the other hand, in the case of spin up, $\langle\psi^\Lambda_\uparrow(0)|\hat{x}^j|\psi^\Lambda_\uparrow(0)\rangle$ is expressed as

$$\begin{aligned} &\langle\psi^\Lambda_\uparrow(0)|\hat{x}^j|\psi^\Lambda_\uparrow(0)\rangle \\ &= \cosh\chi \iint dp^1dp^2 F^*_{0,\uparrow}(p^1,p^2)\hat{x}^j F_{0,\uparrow}(p^1,p^2) \\ &= \frac{i}{2}\cosh\chi\left[\iint dp^1dp^2\frac{\partial}{\partial p^j}|F_{0,\sigma}(p^1,p^2)|^2 \right.\\ &\quad \left. + \iint dp^1dp^2 i\frac{\partial\phi(p^1,p^2)}{\partial p^j}|F_{0,\sigma}(p^1,p^2)|^2\right]. \end{aligned}$$

The term $|F_{0,\uparrow}(p^1,p^2)|^2$ is also an even function of p^1 and p^2. Furthermore, the partial derivatives of it are odd functions. The partial derivatives of the phase $\phi(p^1,p^2)$ are

$$\frac{\partial\phi(p^1,p^2)}{\partial p^1} = -\frac{p^2}{|\vec{p}\,|^2}, \quad \frac{\partial\phi(p^1,p^2)}{\partial p^2} = \frac{p^1}{|\vec{p}\,|^2}, \tag{F1}$$

where $|\vec{p}\,|^2 = \sqrt{(p^1)^2+(p^2)^2}$. Thus, the integration over p^1 and p^2 gives zero. We next evaluate the first term of $\mathsf{V}_{{\rm cov},jk}$:

$$\begin{aligned} {\rm tr}[\rho^\Lambda(\theta)\hat{x}^j\hat{x}^k] &= \sum_\sigma \langle\psi^\Lambda_\sigma(\theta)|\hat{x}^j\hat{x}^k|\psi^\Lambda_\sigma(\theta)\rangle \\ &= \sum_\sigma \langle\psi^\Lambda_\sigma(0)|(\hat{x}^j-\theta_j)(\hat{x}^k-\theta_k)|\psi^\Lambda_\sigma(0)\rangle \\ &= \sum_\sigma \langle\psi^\Lambda_\sigma(0)|\hat{x}^j\hat{x}^k|\psi^\Lambda_\sigma(0)\rangle + \theta_j\theta_k. \end{aligned}$$

We will calculate each spin-up and -down case separately. After lengthy yet elementary steps, we have

$$\begin{aligned} &\langle\psi^\Lambda_\downarrow(0)|\hat{x}^j\hat{x}^k|\psi^\Lambda_\downarrow(0)\rangle \\ &= -\cosh\chi\iint dp^1dp^2 F_{0,\downarrow}(p^1,p^2)\frac{\partial^2}{\partial p^j\partial p^k}F_{0,\downarrow}(p^1,p^2) \\ &= -\cosh\chi\iint dp^1dp^2 \\ &\quad\times\left[\cos^2\frac{\alpha}{2}\varphi_0(p^1,p^2)\frac{\partial^2}{\partial p^j\partial p^k}\varphi_0(p^1,p^2)\right. \\ &\quad + \frac{1}{2}\frac{\partial}{\partial p^j}\left(\cos^2\frac{\alpha}{2}\right)\frac{\partial}{\partial p^k}[\varphi_0(p^1,p^2)]^2 \\ &\quad \left.+ [\varphi_0(p^1,p^2)]^2\cos\frac{\alpha}{2}\frac{\partial^2}{\partial p^j\partial p^k}\cos\frac{\alpha}{2}\right] \\ &= -\cosh\chi\iint dp^1dp^2 \\ &\quad\times\left[\cos^2\frac{\alpha}{2}\varphi_0(p^1,p^2)\frac{\partial^2}{\partial p^j\partial p^k}\varphi_0(p^1,p^2)\right. \\ &\quad + \frac{1}{2}\frac{\partial}{\partial p^j}\left(\cos^2\frac{\alpha}{2}\right)\frac{\partial}{\partial p^k}[\varphi_0(p^1,p^2)]^2 \\ &\quad \left.+[\varphi_0(p^1,p^2)]^2\left(\frac{1}{2}\frac{\partial^2}{\partial p^j\partial p^k}\cos^2\frac{\alpha}{2} - \frac{\partial\cos\frac{\alpha}{2}}{\partial p^j}\frac{\partial\cos\frac{\alpha}{2}}{\partial p^k}\right)\right] \end{aligned}$$

for the spin-down case and

$$\begin{aligned} &\langle\psi^\Lambda_\uparrow(0)|\hat{x}^j\hat{x}^k|\psi^\Lambda_\uparrow(0)\rangle \\ &= -\cosh\chi\iint dp^1dp^2 F^*_{0,\uparrow}(p^1,p^2)\frac{\partial^2}{\partial p^j\partial p^k}F_{0,\uparrow}(p^1,p^2) \\ &= -\cosh\chi\iint dp^1dp^2 \\ &\quad\times\left[\sin^2\frac{\alpha}{2}\varphi_0(p^1,p^2)\frac{\partial^2}{\partial p^j\partial p^k}\varphi_0(p^1,p^2)\right. \end{aligned}$$

$$+\frac{1}{2}\frac{\partial}{\partial p^j}\left(\sin^2\frac{\alpha}{2}\right)\frac{\partial}{\partial p^k}[\varphi_0(p^1,p^2)]^2$$
$$+[\varphi_0(p^1,p^2)]^2 e^{-i\phi}\sin\frac{\alpha}{2}\frac{\partial^2}{\partial p^j\partial p^k}\left(e^{i\phi}\sin\frac{\alpha}{2}\right)\Bigg]$$
$$=-\cosh\chi\iint dp^1dp^2$$
$$\times\Bigg[\sin^2\frac{\alpha}{2}\varphi_0(p^1,p^2)\frac{\partial^2}{\partial p^j\partial p^k}\varphi_0(p^1,p^2)$$
$$+\frac{1}{2}\frac{\partial}{\partial p^j}\left(\sin^2\frac{\alpha}{2}\right)\frac{\partial}{\partial p^k}[\varphi_0(p^1,p^2)]^2$$
$$+[\varphi_0(p^1,p^2)]^2\left(\frac{1}{2}\frac{\partial^2}{\partial p^j\partial p^k}\sin^2\frac{\alpha}{2}-\frac{\partial\sin\frac{\alpha}{2}}{\partial p^j}\frac{\partial\sin\frac{\alpha}{2}}{\partial p^k}\right.$$
$$\left.-\frac{\partial\phi}{\partial p^j}\frac{\partial\phi}{\partial p^k}\sin^2\frac{\alpha}{2}\right)\Bigg]$$

for the spin-up case. Note that the last term does not appear in the spin-down case. All other terms vanish upon integrating over p^1 and p^2 due to oddness of the integrands. Combining the two contributions gives

$$\sum_\sigma\langle\psi^\Lambda_\sigma(0)|\hat{x}^j\hat{x}^k|\psi^\Lambda_\sigma(0)\rangle$$
$$=-\cosh\chi\iint dp^1dp^2\Bigg[\varphi_0(p^1,p^2)\frac{\partial^2}{\partial p^j\partial p^k}\varphi_0(p^1,p^2)$$
$$-[\varphi_0(p^1,p^2)]^2\left(\frac{\partial\cos\frac{\alpha}{2}}{\partial p^j}\frac{\partial\cos\frac{\alpha}{2}}{\partial p^k}+\frac{\partial\sin\frac{\alpha}{2}}{\partial p^j}\frac{\partial\sin\frac{\alpha}{2}}{\partial p^k}\right.$$
$$\left.+\frac{\partial\phi}{\partial p^j}\frac{\partial\phi}{\partial p^k}\sin^2\frac{\alpha}{2}\right)\Bigg]$$
$$=-\cosh\chi\iint dp^1dp^2\Bigg[\varphi_0(p^1,p^2)\frac{\partial^2}{\partial p^j\partial p^k}\varphi_0(p^1,p^2)$$
$$-[\varphi_0(p^1,p^2)]^2$$
$$\times\left(\frac{1}{\sin^2\alpha}\frac{\partial\cos\alpha}{\partial p^j}\frac{\partial\cos\alpha}{\partial p^k}+\frac{\partial\phi}{\partial p^j}\frac{\partial\phi}{\partial p^k}\sin^2\frac{\alpha}{2}\right)\Bigg].$$

We use

$$\frac{1}{2}\frac{\partial}{\partial p^j}\left(\cos^2\frac{\alpha}{2}+\sin^2\frac{\alpha}{2}\right)\frac{\partial}{\partial p^k}[\varphi_0(p^1,p^2)]^2=0. \tag{F2}$$

The first integration without a factor $\cosh\chi$ is nothing but the nonrelativistic case and is given by $\delta_{jk}\kappa^2/2$, which is equal to the inverse of the SLD Fisher information matrix in the rest frame. The second and third integrations are calculated as

$$\iint dp^1dp^2[\varphi_0(p^1,p^2)]^2\frac{1}{\sin^2\alpha}\frac{\partial\cos\alpha}{\partial p^j}\frac{\partial\cos\alpha}{\partial p^k}$$
$$=\delta_{jk}\frac{\kappa^2V^2}{4}$$
$$\times\int_0^\infty dt\frac{tm^2}{(t^2+m^2)(\sqrt{t^2+m^2}+m\sqrt{1-V^2})^2}e^{-\kappa^2t^2}$$
$$=\delta_{jk}\frac{\kappa^2}{2}\frac{V^2}{2}\mu_1\iint dp^1dp^2[\varphi_0(p^1,p^2)]^2\frac{\partial\phi}{\partial p^j}\frac{\partial\phi}{\partial p^k}\sin^2\frac{\alpha}{2}$$
$$=\iint dp^1dp^2[\varphi_0(p^1,p^2)]^2\frac{p^jp^k}{|p|^4}\frac{1-\cos\alpha}{2}$$
$$=\delta_{jk}\frac{\kappa^2}{2}\left(1-\frac{1}{\cosh\chi}\right)$$
$$\times\int_0^\infty dt\frac{\sqrt{t^2+m^2}-m}{\sqrt{t^2+m^2}+m\sqrt{1-V^2}}e^{-\kappa^2t^2}$$
$$=\delta_{jk}\frac{\kappa^2}{2}(1-\sqrt{1-V^2})\mu_2.$$

By changing the integration variables, we get the same expressions as in the main text.

[1] D. Harlow, Rev. Mod. Phys. **88**, 015002 (2016).
[2] J. Maldacena, Nat. Rev. Phys. **2**, 123 (2020).
[3] P. M. Alsing, D. McMahon, and G. J. Milburn, J. Opt. B **6**, S834 (2004).
[4] D. E. Bruschi, J. Louko, E. Martín-Martínez, A. Dragan, and I. Fuentes, Phys. Rev. A **82**, 042332 (2010).
[5] D. Hosler and P. Kok, Phys. Rev. A **88**, 052112 (2013).
[6] Y. Yao, X. Xiao, L. Ge, X. G. Wang, and C. P. Sun, Phys. Rev. A **89**, 042336 (2014).
[7] P. M. Alsing, I. Fuentes-Schuller, R. B. Mann, and T. E. Tessier, Phys. Rev. A **74**, 032326 (2006).
[8] D. Ahn, H. J. Lee, Y. H. Moon, and S. W. Hwang, Phys. Rev. A **67**, 012103 (2003).
[9] H. Terashima and M. Ueda, Quantum Inf. Comput. **3**, 224 (2003).
[10] H. Terashima and M. Ueda, Int. J. Quantum Inf. **01**, 93 (2003).
[11] Y. H. Moon, D. Ahn, and S. W. Hwang, Prog. Theor. Phys. **112**, 219 (2004).
[12] S. Moradi, Phys. Rev. A **77**, 024101 (2008).
[13] P. Caban, J. Rembieliński, and M. Włodarczyk, Phys. Rev. A **79**, 014102 (2009).
[14] A. Peres, P. F. Scudo, and D. R. Terno, Phys. Rev. Lett. **88**, 230402 (2002).
[15] D. R. Terno, Phys. Rev. A **67**, 014102 (2003).
[16] P. M. Alsing and G. J. Milburn, Quantum Inf. Comput. **2**, 487 (2002).
[17] A. Peres and D. R. Terno, Int. J. Quantum Inf. **01**, 225 (2003).
[18] S. Weinberg, *The Quantum Theory of Fields* (Cambridge University Press, Cambridge, 2005), Vol. 1.
[19] F. R. Halpern, *Special Relativity and Quantum Mechanics* (Prentice-Hall, Englewood Cliffs, 1968).
[20] R. M. Gingrich and C. Adami, Phys. Rev. Lett. **89**, 270402 (2002).
[21] T. F. Jordan, A. Shaji, and E. C. G. Sudarshan, Phys. Rev. A **73**, 032104 (2006).
[22] D. Lee and E. C. Young, New J. Phys. **6**, 67 (2004).
[23] J. Pachos and E. Solano, Quantum Inf. Comput. **3**, 115 (2003).

[24] L. Lamata, M. A. Martin-Delgado, and E. Solano, Phys. Rev. Lett. **97**, 250502 (2006).
[25] A. Peres and D. R. Terno, Rev. Mod. Phys. **76**, 93 (2004).
[26] N. Friis, R. A. Bertlmann, M. Huber, and B. C. Hiesmayr, Phys. Rev. A **81**, 042114 (2010).
[27] E. Castro-Ruiz and E. Nahmad-Achar, Phys. Rev. A **86**, 052331 (2012).
[28] W. T. Kim and E. J. Son, Phys. Rev. A **71**, 014102 (2005).
[29] A. S. Holevo, *Probabilistic and Statistical Aspects of Quantum Theory*, 2nd ed. (Edizioni della Normale, Pisa, 2011).
[30] C. W. Helstrom, *Quantum Detection and Estimation Theory* (Academic, New York, 1976).
[31] S. L. Braunstein, C. M. Caves, and G. J. Milburn, Ann. Phys. (NY) **247**, 135 (1996).
[32] M. Ahmadi, M., D. E. Bruschi, C. Sabín, G. Adesso, and I. Fuentes, Sci. Rep. **4**, 4996 (2014).
[33] M. Ahmadi, D. E. Bruschi, and I. Fuentes, Phys. Rev. D **89**, 065028 (2014).
[34] Z. Tian, J. Wang, H. Fan, and J. Jing, Sci. Rep. **5**, 7946 (2015).
[35] X. Liu, J. Jing, Z. Tian, and W. Yao, Phys. Rev. D **103**, 125025 (2021).
[36] P. Caban, J. Rembieliński, and M. Włodarczyk, Ann. Phys. (NY) **330**, 263 (2013).
[37] A. Fujiwara and H. Nagaoka, Phys. Lett. A **201**, 119 (1995).
[38] J. Suzuki, Y. Yang, and M. Hayashi, J. Phys. A: Math. Theor. **53**, 453001 (2020).
[39] S. Ragy, M. Jarzyna, and R. Demkowicz-Dobrzański, Phys. Rev. A **94**, 052108 (2016).
[40] J. Suzuki, Entropy **21**, 703 (2019).
[41] J. J. Sakurai and J. Napolitano, *Modern Quantum Mechanics*, 3rd ed. (Cambridge University Press, Cambridge, 2020).
[42] J. Liu, H. Yuan, X. M. Lu, and X. Wang, J. Phys. A: Math. Theor. **53**, 023001 (2019).